第28卷 第12期
2007年12月

半 导 体 学 报
CHINESE JOURNAL OF SEMICONDUCTORS

Vol.28 No.12
Dec.,2007

The Bipolar Field-Effect Transistor: II. Drift-Diffusion Current Theory (Two-MOS-Gates on Pure-Base) *

Chih-Tang Sah[1,2,3,†] and Bin B. Jie[3,†]

(1 *Chinese Academy of Sciences*, *Foreign Member*, *Beijing* 100864, *China*)
(2 *University of Florida*, *Gainesville*, *Florida* 32605, *USA*)
(3 *Peking University*, *Beijing* 100084, *China*)

Abstract: This paper describes the drift-diffusion theory of the bipolar field-effect transistor (BiFET) with two identical and connected metal-oxide-silicon-gates (MOS-gates) on a thin-pure-base. Analytical solution is obtained by partitioning the two-dimensional transistor into two one-dimensional problems coupled by the parametric surface-electric-potential. Total and component output and transfer currents and conductances versus D.C. voltages from the drift-diffusion theory, and their deviations from the electrochemical (quasi-Fermi) potential-gradient theory, are presented over practical ranges of thicknesses of the silicon base and gate oxide. A substantial contribution from the longitudinal gradient of the square of the transverse electric field is shown.

Key words: bipolar field-effect transistor theory; MOS field-effect transistor; simultaneous electron and hole surface and volume channels; surface potential; longitudinal gradient of transverse electric field

PACC: 7340Q **EEACC**: 2560S; 2560B

CLC number: TN386.1 **Document code**: A **Article ID**: 0253-4177(2007)12-1849-11

1 Introduction

The silicon MOS field-effect transistor technology is advancing towards the nanometer range in the form of double-gate and thin pure-base, fin-like structure, known as the FinFET[1]. Their experimental electrical current-voltage characteristics, recently reported by IMEC with 4-company assignees[2], could not be accounted for by the traditional unipolar field-effect theory, invented by Shockley in 1952 and followed by recent device theorists and engineers, such as those reviewed by Ortiz-Conde−Garcia-Sanchez−Liou[3]. It was recently demonstrated by us[4~7] that the observed experimental current-voltage characteristics reported by IMEC+Assignees[2] showed distinct bipolar behavior, namely the simultaneous presence of both electron and hole surface-inversion-channel currents, even a hint of volume-channel currents, giving six channels in their two-MOS-gates on thin-base FinFET structures. The IMEC data covered wide ranges of oxide and base thicknesses and gate or base lengths, and also drain-source contact types, giving confidence that first-silicon random variations observed in the data do not mask the observed current voltage characteristics that pointed to the bipolar nature in these FinFETs. We named the discovery of the bipolar nature of the FET and its theory, the Bipolar Field Effect Transistor (BiFET) Theory[4~7], to replace Shockley's 1952 Unipolar Field-Effect Transistor Theory (UniFET). Such a bipolar FET characteristic in one transistor structure was conceived as early as 1970 by a complementary pair of FETs and experimentally demonstrated in 1971-Fu-Sah[8], showing bistable negative conductance *I-V* characteristics in a FET containing a surface-inversion-channel pMOST in the n-basewell on a p-Si substrate, and a n-volume-channel nJGFET (n-basewell/p-substrate Junction-Gate FET).

In our previous report[7], we presented the electrochemical-potential-gradient driven current theory for the two-MOS-gates on pure-base silicon BiFET, using the classical parametric surface-potential approach given in 1966-Sah-Pao[9,10]. This present paper describes the more popular drift-diffusion current theory, which is as exact as the electrochemical potential gradient current theo-

* This investigation and Binbin Jie have been supported by the CTSAH Associates (CTSA) founded by the late Linda Su-Nan Chang Sah.
† Corresponding author. Email: bb_jie@msn.com and tom_sah@msn.com
Received 31 October 2007, revised manuscript received 10 November 2007

ry[4~7]. In this drift-diffusion current theory, the drift and diffusion current components are further decomposed into subcomponents. These subcomponents are similar to the subcomponents shown by us for the single-MOS-gate thick impure-base FET reported in Refs. [13, 14]. The analytical formulas of the subcomponents of the drift and diffusion currents were rigorously derived by Sah in 1996-Sah[15] for the single-MOS-gate on thick impure-base unipolar field-effect transistor which included also the 2-dimensional terms. These rigorous 1996-Sah formulas were verified mathematically by Jie in 2005-Jie-Sah[13] and 2007-Jie-Sah[14]. In this present paper, the 1996-Sah 4-component drift-diffusion UniFET theory[13~15] is extended to the two-MOS-gates on thin pure-base BiFET or the FinFET. We also present the computed deviations of the drift-diffusion current components from those computed from the electrochemical current theory presented in the first report of this series[7], similar to the deviations computed for the single-gate on thick impure-base in 2007-Jie-Sah[14]. The present deviations are of numerical origin from the complicated numerical integration formulas of the component terms in the drift-diffusion theory. In this paper, we present graphs of sample families of transfer and output current-voltage and conductance-voltage characteristics, (I_D-V_{GS}), (I_D-V_{DS}), (g_{ms}-V_{GS}), (g_{ms}-V_{DS}), (g_{ds}-V_{GS}) and (g_{ds}-V_{DS}), their drift and diffusion components, and their deviations from the electrochemical current theory[7]. Especially important is the discovery of the substantial added-on contribution (~25%) to each of the electron and hole channel currents in the 2-gate-pure-base BiFET from the longitudinal gradient (y-direction is longitudinal to the channel current flow direction) of the square of the transverse electric field, to be denoted as $(\partial/\partial y)(E_X)^2$ or abbreviated to just $(E_X)^2$. This suggests that the neglected $(E_X)^2$ term could also account for the 2% to 5% missing current observed in the 4-component drift-diffusion theory of bulk transistor with one gate and semi-infinite base-body[13,14,16]. This small (2% ~ 5%) missing current was originally attributed by us entirely to the approximation of x-independent longitudinal electric field, $E_Y(x,y) \cong E_Y(x=0, y)$[11,13,14]. which was commonly known as the charge-sheet approximation[12], a misnomer[11].

2 Drift and Diffusion Theory of the Two-Gate on Pure-Base Transistors

The voltage and current equations of the drift-diffusion theory of the UniFET with single-gate on thick or semi-infinite impure-base from 1996-Sah[13~15] are modified for the BiFET with two identical gates on a thin pure-base[4~7]. They are summarized as follows. The variables are functions of the 2-dimensional coordinates (x, y) with no variation along the width of the gate and channel in the z-direction from $z=0$ to $z=Z=W$. The y-axis is the direction of the channels and the x-axis, the SiO_2/Si interfacial planes of the two gates, located at $x=0$ and $x=x_B$ with base thickness x_B. The two gate oxides have equal electrical thickness of x_O. The impurity concentration in the pure base is zero, $P_{IM}=0$. The concentrations of the traps or generation-recombination-trapping centers are also assumed zero in both the pure-base and at the two gate-oxide/pure-base interfaces. The source and drain contacts to the pure-base are located respectively at $y=0$ and $y=L$. The effects from the contacts will be considered in the fifth report of this 5-report series. The three potential variables are normalized to kT/q and denoted by $U_\alpha = qV_\alpha/kT$ where respectively, α = N, P, and I are for the electron and hole electrochemical, and the electric potentials and I for midgap or intrinsic is usually omitted. Near thermal equilibrium (low electric field or no hot carriers) is assumed, so the Einstein relationship between mobility and diffusivity holds for electrons and holes, $D_n/\mu_n = (kT/q)$ and $D_p/\mu_p = (kT/q)$ where $T = T_L$ is the lattice or heat-transfer temperature. The Poisson Equation and the electron and hole current equations are then given by the classical macroscopic equations which are three non-zero equations of the six Shockley Equations of electric charge transport in solids[7]. The terminal currents are denoted by I_T where T = D (drain), S (source), G1 (gate-1), G2 (gate-2), B (Base).

$$\nabla \cdot (\varepsilon_S E) = \rho(x,y,z) = q(P - N - P_{IM}) \quad \text{3-Dimensional Impure}$$

$$= \varepsilon_S[(\partial E_X/\partial x) + (\partial E_Y/\partial y)] = q(P - N) \quad \text{2-Dimensional Pure} \quad (1)$$

$$= qn_i[\exp(U_P - U) - \exp(U - U_N)] \quad (1A)$$

$$I_{DN} = -(W/L)\iint[q\mu_n NE_Y + qD_n(\partial N/\partial y)]\,\partial x\partial y$$
$$(x = 0 \text{ to } x_B;\ y = 0 \text{ to } L) \quad (2)$$

$$I_{DP} = -(W/L)\iint[q\mu_p PE_Y + qD_p(\partial P/\partial y)]\,\partial x\partial y$$
$$(x = 0 \text{ to } x_B;\ y = 0 \text{ to } L) \quad (3)$$

$$I_D = I_{DN} + I_{DP} = -I_S \quad (4)$$

Following the rigorous derivation algebra given in 1996-Sah[15], the diffusion terms can be readily evaluated and have the linear dependence on the surface potential and applied gate voltages. The drift terms are subject to further tedious algebra as shown in Ref. [15] with the remote boundary condition at $x = \infty$ moved into the symmetry plane, $x = x_B/2$, where only the electric field boundary condition holds, $E_X(x = x_B/2, y) = 0$, not the electrical neutrality. Using $E_X = -(kT/q)(\partial U/\partial x)$ and $E_Y = -(kT/q)(\partial U/\partial y)$, and the x-independent electrochemical potential assumption[4~7,9~11,13~15], expressed by $U_P(x, y) = U_P(y)$ and $U_N(x, y) = U_N(y)$, we get the 1-dimensional (1-D) Gauss Law from converting the volume integration of the Poisson Equation (1) into a surface integration using the divergence theorem $\iiint \nabla \cdot (\varepsilon_O E)\mathrm{d}\mho = \oiint (\varepsilon_O E) \cdot \mathrm{d}S$ with the line integrals $\int (\partial/\partial y)(\varepsilon_O E_Y)\partial x$ ($x = -x_O$ to 0 for MOS gate-1 and x_B to $x_B + x_O$ for MOS gate-2) omitted as next order 2-Dimensional corrections:

$$\varepsilon_S E_X(x = 0, y) = -C_O[V_{GB} - V_{FB} - V(x = 0, y)] \quad (5)$$

$$\varepsilon_S E_X(x = x_B, y) = +C_O[V_{GB} - V_{FB} - V(x = x_B, y)] \quad (6)$$

Using $V(x = 0, y) = V(x = x_B, y) = V_S(y) = U_S(y)(kT/q)$, $V(x = x_B/2, y) = U_0(y)(kT/q)$, and $E_X(x = 0, y) = E_X(x = x_B, y) = E_S(y)$, we get

$$U_{GB} - U_{FB} - U_S = (\mathrm{sign}\,U_S) \times (C_D/C_O) \times \Big\{[\exp(U_S - U_N) - \exp(U_0 - U_N)] + [\exp(U_P - U_S) - \exp(U_P - U_0)]\Big\}^{1/2} \quad (7)$$

$$x_B/L_D \equiv X_B = 2\int(\mathrm{sign}\,U)\Big\{[\exp(U - U_N) - \exp(U_0 - U_N)] + [\exp(U_P - U) - \exp(U_P - U_0)]\Big\}^{-1/2}\partial_X U \quad (8)$$

where the integration is taken from $U = U_0$ to U_S. $L_D = (\varepsilon_s kT/2q^2 n_i)^{1/2}$ is the Debye screening length ~26μm at room temperature. In the electron emitter section[4~7], the electron terms dominate and the hole terms can be neglected as a first approximation. In the hole emitter section[4~7], the hole terms dominate and the electron terms can be neglected as a first approximation. Thus, the first approximation of Eq. (8) in the electron emitter section is given by

$$x_B/L_D \equiv X_B = 2\int(\mathrm{sign}\,U)\Big\{\exp(U - U_N) - \exp(U_S - U_N) + (C_O/C_D)^2(U_{GB} - U_{FB} - U_S)^2\Big\}^{-1/2}\partial_X U \quad (9)$$

where the integration is from $U = U_N + \log_e[\exp(U_S - U_N) - (C_O/C_D)^2(U_{GB} - U_{FB} - U_S)^2]$ to U_S.

In this first attempt of characterization of the bipolar MOSFET, we have assumed that the drain and source regions of the thin pure base are identical, therefore, the use of the words "source" and "drain" to label these two ends of the thin pure-base is entirely arbitrary. Nevertheless, to connect this new bipolar FET to the past unipolar FET terminology coined by Shockley in 1952 and used by all subsequent engineers and scientists until today, we will name them[4~7] as the source electron emitter section which simultaneously is also the source hole collector region. Similarly, the drain electron collector section is simultaneously also the drain hole emitter region. This creates a semantic conflict of the words drain and emitter, and source and collector. Therefore, it may be preferable to discard the arbitrary designation of drain and source at the two ends of the base layer of the bipolar thin-base FET, and retain the bipolar junction transistor (BJT) terminology of emitter and collector, which were also coined by Shockley, in 1949, for the bipolar junction transistor[4~7], noting the only difference between the two is that drift current dominates in the FET operation and diffusion current dominates in the BJT operation, regardless of the conductivity type of the base layer.

The electron emitter section and hole collector section occupy the same physical space of the bipolar field-effect transistor. This is a previously unrecognized cardinal feature of the BiFET or all FETs. Thus, once the hole concentration in the hole collector (electron emitter) drain section is solved, the spatial variation (y-dependence) of the hole quasi-Fermi potential can be computed. The next order solution of the two coupled equations, (7) and (8), is then obtained. If only the dominant carrier terms in either the electron or hole emitter section are kept, U_0 can be eliminated between (7) and (8) to give one gate-voltage-surface-potential equation which can then be solved numerically without iteration as attained by many investigators[3,17].

Following 1996-Sah[15], the current equations (2) and (3) can be manipulated with the help of the bipolar Poisson Equation (1) as follows to give the total drift and diffusion currents and also their components. In the pure-base electron channel used here with the identical double gates, the electron terms dominate, thus, we use Eq.(1) for N in the drift term of Eq.(2), and the integration limits $y=0$ to $y=L$ and $x=0$ to $x=x_B$ where $E_X(x=x_B/2, y)=0$. Then we get

$$-\iint qNE_Y\partial x\partial y = \iint \varepsilon_S[(\partial E_X/\partial x)+(\partial E_Y/\partial y)]E_Y\partial x\partial y$$
$$= C_O\left\{[V_{GB}-V_{FB}-V_S(0)]^2-[V_{GB}-V_{FB}-V_S(L)]^2\right\}+$$
$$\iint(\partial/\partial y)(E_Y{}^2/2)\partial x\partial y+\iint(\partial/\partial y)(-E_X{}^2/2)\partial x\partial y \quad (10)$$

It is important to note that the first double integral $\iint(\partial/\partial y)(E_Y{}^2/2)\partial x\partial y$ is the short-channel drift current correction term, which is reported in a future paper, while the second double integral $\iint(\partial/\partial y)(E_X{}^2/2)\partial x\partial y$ is a long-channel drift current term, which is independent of channel length. It is the longitudinal gradient of the square of the transverse electric field mentioned earlier and in the abstract. It can be evaluated analytically to give three components which are:

$$\iint(\partial/\partial y)(-E_X{}^2/2)\partial x\partial y = +2(kT/q)C_O[V_S(L)-V_S(0)] \quad \text{linear term}$$
$$+C_O(X_B/2)(C_O/C_D)\left\{[V_{GB}-V_{FB}-V_S(0)]^2-[V_{GB}-V_{FB}-V_S(L)]^2\right\} \quad \text{parabolic term}$$
$$+C_O(X_B/2)(C_D/C_O)(kT/q)^2\left\{\exp[U_S(L)-U_N(L)]-\exp[U_S(0)-U_S(0)]\right\} \quad \text{exponential term}$$
$$(11)$$

Collecting the above into the electron channel current equation (2), we obtain (with $U_{SB}=0$)

$$I_N=\mu_n(W/L)\times C_O(kT/q)^2\Big\{[U_{GB}-U_{FB}-U_S(0)]^2-[U_{GB}-U_{FB}-U_S(L)]^2+2[U_S(L)-U_S(0)]+(X_B/2)(C_O/C_D)\times[(U_{GB}-U_{FB}-U_S(0))^2-(U_{GB}-U_{FB}-U_S(L))^2]+(X_B/2)(C_D/C_O)[\exp(U_S(L)-U_N(L))-\exp(U_S(0)-U_N(0))]\Big\}+D_n(W/L)\times 2C_O(kT/q)[U_S(L)-U_S(0)] \quad (12)$$

The same procedure gives the hole channel current (with $V_{DB}=0$ as the reference).

$$I_P=\mu_p(W/L)\times C_O(kT/q)^2\Big\{[U_{GB}-U_{FB}-U_S(0)]^2-[U_{GB}-U_{FB}-U_S(L)]^2+2[U_S(L)-U_S(0)]+(X_B/2)(C_O/C_D)[(U_{GB}-U_{FB}-U_S(0))^2-(U_{GB}-U_{FB}-U_S(L))^2]+(X_B/2)(C_D/C_O)[\exp(U_P(L)-U_S(L))-\exp(U_P(0)-U_S(0))]\Big\}+D_p(W/L)\times 2C_O(kT/q)[U_S(L)-U_S(0)] \quad (13)$$

The total channel current or the drain and source terminal currents of the bipolar field-effect transistor with two identical MOS gates are then given by the sum $I_N+I_P=I_D=-I_S$. These are exactly those obtained in the 1996-Sah space-charge theory[15] with four current-components (P_1, P_2, D_1 and D_2), which is reduced to two (P_1 and D_1) because of pure base with $P_{IM}=0$ and which uses the boundary condition at $x=x_B/2$ to obtain the surface potential at the oxide/silicon interface, $V(x=0,y)=V_S(y)=(kT/q)U_S(y)$ which appeared in Eq.(9).

3 Computed Current- and Conductance-Voltage Characteristics

In order to provide in one article all the important characteristics that may be needed by compact model developing engineers to assess the accuracy of their approximations, we shall present the computed characteristics in 18 figures as self-explainable as possible, each with three or two parts, consisting of the total value, the drift and

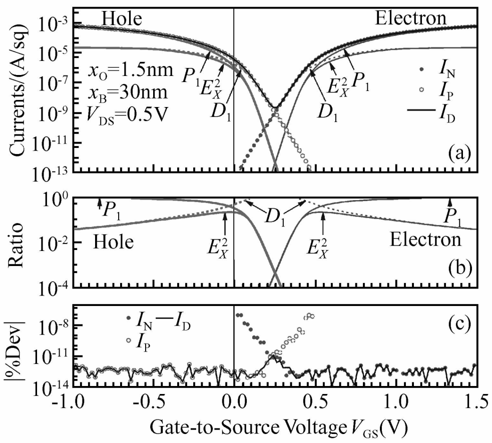

Fig. 1　Gate-source voltage V_{GS} dependence of the DC current of an nFinFET or the transfer characteristics. (a) Total drain terminal current I_D and the electron and hole drift and diffusion channel current components. (b) The fraction of the parabolic drift current P_1, diffusion current D_1, and the $(\partial/\partial y)(E_X)^2$ components of the total current I_D. (c) The percentage deviation of the electron I_N and hole I_P, and total I_D currents from their electrochemical potential gradient values.

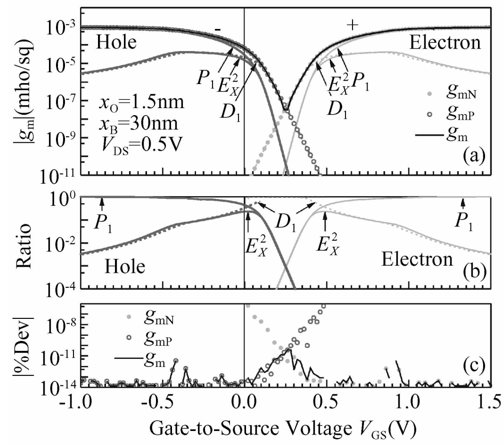

Fig. 2　Same as Figs. 1 (a), 1 (b) and 1 (c) except the currents are replaced by the transconductances, g_m.

diffusion component values, and the percentage deviation of the drift-diffusion values from the electrochemical potential-gradient values computed previously[7]. The first three figures give the three transfer characteristics, drain current, drain conductance and transconductance as a function of the gate voltage. The second three figures give the three output characteristics, drain current, drain conductance and transconductance as a function of the drain voltage. The source is tied to the reference denoted by base or B, so $V_{SB}=0$. This distinguishes the previously not recognized property which is central to the bipolar nature and operation of the MOSFET[4], namely, the threshold gate voltage at the source is $V_{GSth} = V_{GBth} - V_{SB}$ while the threshold gate voltage at the drain is $V_{GDth} = V_{GBth} - V_{DB}$. This recognition first described in Ref. [4] allowed the solutions to be applied at once to both the electron and the hole channels[5~7] with only a simple change of symbols, signs, and reference voltages. The remaining twelve figures, Figs. 7 to 18, show the very significant contributions (as much as 25%) to the channel currents and conductances from the long-channel (or channel-length-independent) longitudinal-gradient of the square of the transverse electric field, $(\partial/\partial y)(E_X)^2$. This was not recognized in both the past theory of the single-gate on semi-infinite-thick impure-base[9~16] and the recent theory of double-gate on thin pure-base[2~7,17]. The effects of longitudinal electric field, E_Y, from the same origin with the same form, $(\partial/\partial y)(E_Y)^2$, was well-known for the single-gate semi-infinite-thick impure-base, described in 1990-Mitiko-Miura-Mattausch[18] and rigorously derived in 1996-Sah[15]. It is channel-length dependent and its analysis is deferred to a future report on the two-section model for the short channels[4~7]. The characteristics given by these 18 figures will now be discussed.

Figure 1 gives the transfer characteristics, with $V_{SB}=0$ or the source as the reference. Figure 1 (a) shows the total drain current and its drift and diffusion components in the electron and hole channels. Figure 1 (b) shows the fractional contribution to the total current (or their ratios to the total electron or hole channel current) of the parabolic drift P_1 and linear diffusion D_1 current components, and the previously not recognized large contribution from the longitudinal-gradient term $(\partial/\partial y)(E_X)^2$ which reaches ~25% around the electron and hole threshold voltages defined previously by us for pure-base[7] ($V_{GS}\sim +0.5$V and 0.0V). Figure 1 (c) shows the excellent accuracy ($<10^{-11}$% deviation at $I_{Dmin}=2\times10^{-9}$ A/sq at $V_{GS}=+0.25$V) in both the electron and hole channel currents in the entire operation range, V_{GS} or $V_{GB}=-1.0$V to $+1.5$V. Note the approximate threshold voltages of the pMOST and the nMOST of $+0.5$V shifted by the applied

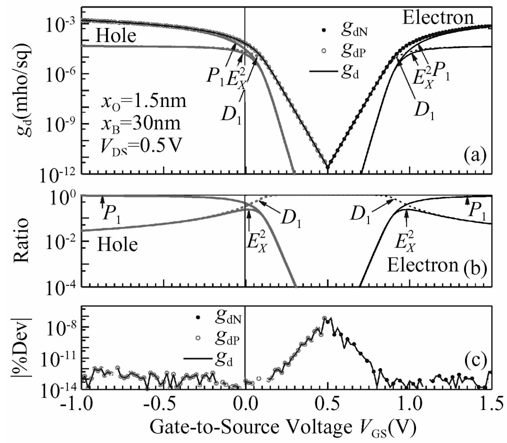

Fig. 3 Same as Fig. 2 except the output or drain conductance g_d is shown. However, note that the minimum of the V-shaped curve is shifted to $V_{GS} = +0.5V$ instead of $+0.25V$ of Figs. 1 and 2 because the channels are in or out of the drain current saturation range of the V_{GS} bias range at the fixed $V_{DS} = +0.5V$.

source-drain voltage of $+0.5V$, which is defined by us previously[7] from the oxide and Debye screening capacitance ratio, $V_{GBth} = 2(kT/q) \times \log_e(C_O/C_D) \sim +0.5V$. Thus, the hole channel threshold voltage is $V_{GDth\text{-}hole} = V_{GBth} - V_{DB} = +0.5 - 0.5V = 0.0V$ and the electron channel threshold voltage is $V_{GSth\text{-}electron} = V_{GBth} - V_{SB} = +0.5 - 0.0V = +0.5V$ which are confirmed in Figs. 1 (a) and

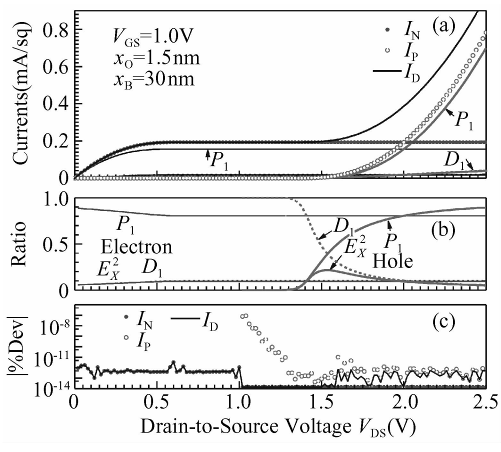

Fig. 4 Drain-source voltage V_{DS} dependence of the DC current of an nFinFET or the output characteristics. The three parts, 4 (a), 4 (b) and 4 (c), are similar to those in Figs. 1 (a), 1 (b) and 1 (c). Note a most important feature, that is, the onset of the hole channel current at $V_{DS} = +1.5V$ because $V_{GS} = +1.0V$, or $V_{DS} \geqslant V_{DS\text{-sat}} = V_{GS} + V_{GS\text{-th}}$ in the hole channel current 'saturation' range.

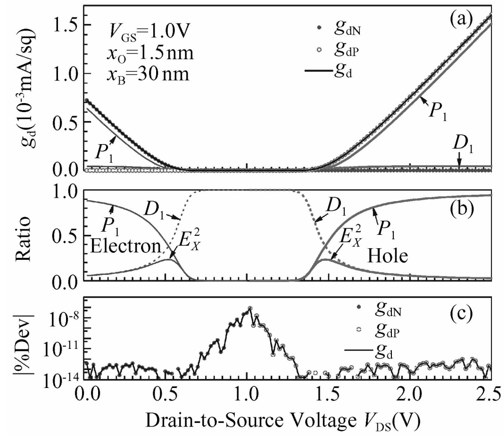

Fig. 5 Same as Fig. 4 but for output or drain conductance, g_d. The three parts, 5 (a), 5 (b) and 5 (c), are similar to those in Figs. 3 (a), 3 (b) and 3 (c). In the drain-current saturation range, g_d decreases exponentially with V_{DS}, similar to its exponential decrease with V_{GS} in the non-saturation or parabolic range shown in Fig. 3 (a).

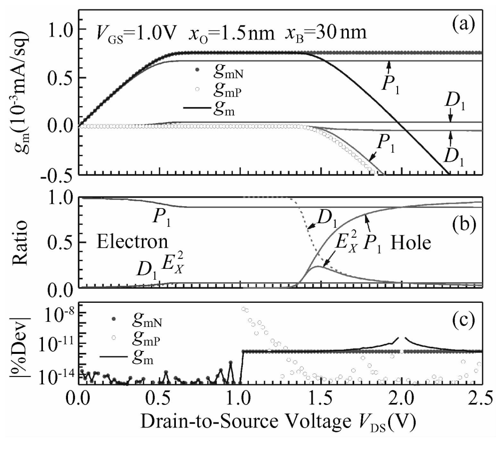

Fig. 6 Drain-source voltage V_{DS} dependence of the transconductance, g_m. The three parts, 6 (a), 6 (b) and 6 (c), are similar to those in Figs. 2 (a), 2 (b) and 2 (c). In the drain-electron-current saturation range, and drain hole-current exponentially rising, g_{mN} from the electron channel saturates to a constant value, while g_{mP} from the hole channel increases exponentially with V_{DS}, from $V_{DS} = 0$ to $V_{DSsat} = V_{GS} + V_{GSth} = 1.0 + 0.5 = +1.5V$, then parabolically with further increasing $V_{DS} > V_{DS\text{-sat}}$ in which V_{GD} also increases with V_{DS} to keep the hole channel continually at the hole-channel-current at the saturation point, giving the parabolic rise of the hole channel and hole transconductance, $g_{mP} \propto (V_{DS} + V_{DSsat})^2$, obtained in the 1964-Sah theory of pure-base or voltage-independent-base-impurity-(or bulk)-charge.

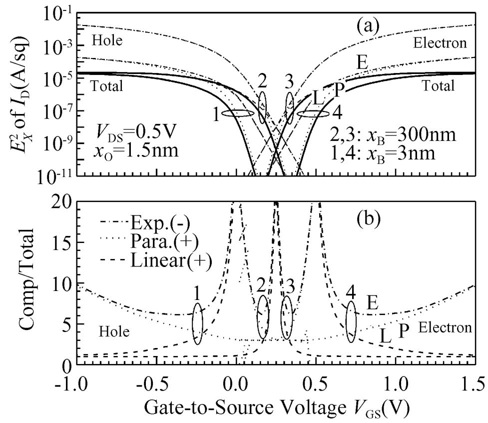

Fig. 7　Effects of base thickness, x_B = 3nm and 300nm, on the contributions of the three $(E_X)^2$ terms, Exponential, Parabolic, and Linear to the electron and hole channel currents. (a) Similar to that given in Fig. 1 (a) except that the three $(\partial/\partial y)(E_X)^2$ terms are given in place of the drift and diffusion components. (b) The contributions of the three terms of $(\partial/\partial y)(E_X)^2$ as a fraction of the total $(\partial/\partial y)\times(E_X)^2$ contributions. Note the near complete cancellation of the parabolic and exponential $(\partial/\partial y)(E_X)^2$ terms in the subthreshold range $0 < V_{GS} < +0.5$V, and the linear and exponential $(\partial/\partial y)(E_X)^2$ terms in the strong channel current range, $V_{GS}<0$ for the hole channel and $V_{GS}> +0.5$V for the electron channel.

1 (b). Figure 1 (b) shows that these threshold voltages are also where the $(\partial/\partial y)(E_X)^2$ contribution to the channel current peaks. Our assumption of identical electron and hole mobilities gives the V-shaped I_D-V_{GS} with the mirror image plane centrally located between the electron and hole threshold voltages: $I_{D\text{-min}}$ at $V_{GS\text{-min}} = V_{DS}/2 = +0.25$V as illustrated in Fig. 1 (a).

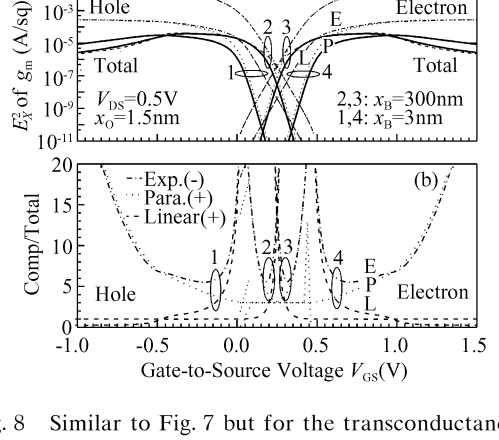

Fig. 8　Similar to Fig. 7 but for the transconductance, g_m.

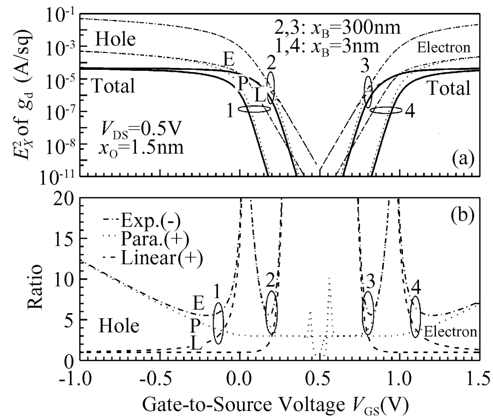

Fig. 9　Similar to Fig. 8 but for the output or drain conductance, g_d.

Figure 2 (a) gives the transconductance and its dominant drift component in the strong surface channel range, $V_{GS} < -0.25$V from holes, and $V_{GS} > +0.75$V from electrons, and its dominant diffusion component in the subthreshold surface channel range, $+0.15\text{V} < V_{GS} < +0.25$V from holes and $+0.25\text{V} < V_{GS} < +0.35$V from electrons. Figure 2 (b) gives the fraction of the dominant parabolic drift current P_1, linear diffusion current D_1, and $(\partial/\partial y)(E_X)^2$ current, in the voltage ranges corresponding to those in Fig. 2 (a).

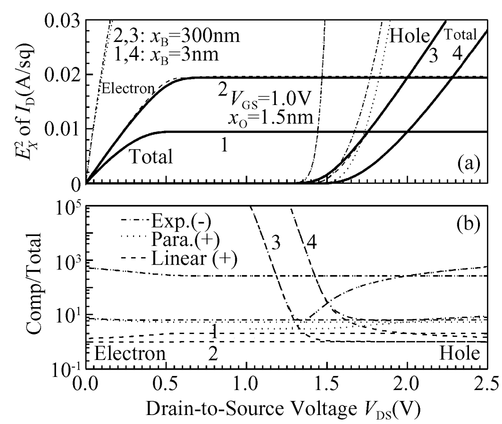

Fig. 10　These two parts of the figure are similar to those in Fig. 7. They give the effects of base thickness, x_B = 3nm and 300nm, on the contributions from three $(\partial/\partial y)(E_X)^2$ terms, Exponential, Parabolic, and Linear, to the electron and hole channel currents. (a) Similar to that given in Fig. 4 (a) except that the three $(\partial/\partial y)(E_X)^2$ terms (linear, parabolic, and exponential) are shown in place of the drift and diffusion components. (b) The contributions of the three components of the $(\partial/\partial y)(E_X)^2$ as a fraction of the total $(\partial/\partial y)(E_X)^2$ contributions.

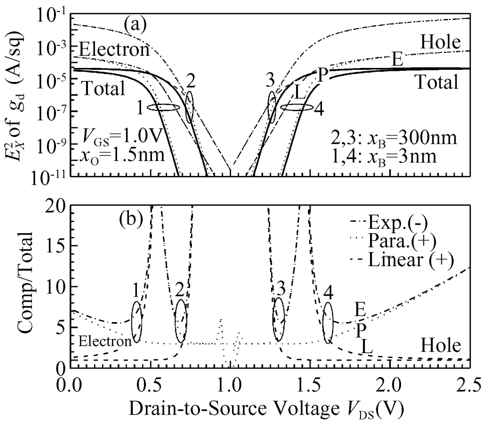

Fig. 11 Similar to Fig. 10 but for the output or drain conductance, gd.

Figure 2 (c) gives the percentage deviation of the electron and hole channel transconductance from their electrochemical-potential-gradient values computed previously[7], showing less than 10^{-14}% in the strong channel current range and less than 2×10^{-11}% in the subthreshold current range and at the minimum $g_m = 2\times10^{-8}$ ℧/sq at V_{GS} = +0.25V.

Figures 3 (a), 3 (b) and 3 (c) show the gate voltage dependence of drain-source terminal conductance and its components, similar to the corresponding Figs. 2 (a), 2 (b) and 2 (c) for the transconductance and its components just described. The larger deviations of the electron and hole channel conductances are again present in their subthreshold ranges where the second carrier species contributes, but the deviations are still very small, 1.0×10^{-7}% at the minimum $g_d = 1\times10^{-12}$ ℧/sq at V_{GS} = +0.50V.

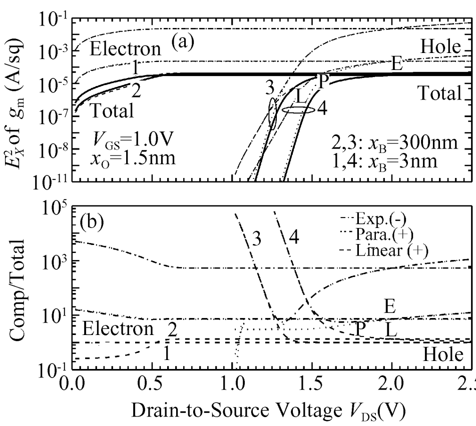

Fig. 12 Similar to Fig. 11 but for transconductance, g_m.

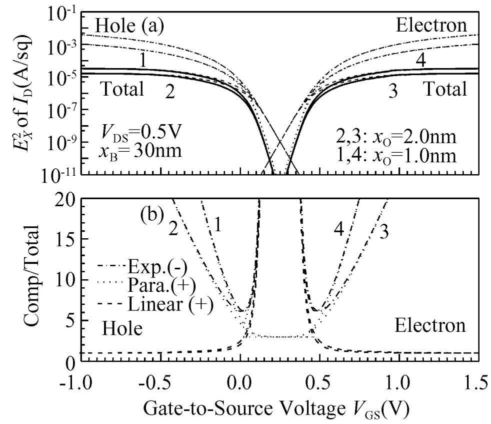

Fig. 13 Effects of oxide thickness, x_O = 1.0nm and 2.0nm, on the contributions of the three $(\partial/\partial y)\times(E_X)^2$ components, Exponential, Parabolic, and Linear to the electron and hole channel current. (a) Similar to that given in Fig. 1 (a) except that the $(\partial/\partial y)(E_X)^2$ terms are shown in place of the drift and diffusion components. (b) The contributions of the three components of the $(\partial/\partial y)(E_X)^2$ (linear, parabolic, and exponential) as a fraction of the total $(\partial/\partial y)(E_X)^2$. Note the cancellation of the parabolic and exponential $(\partial/\partial y)(E_X)^2$ terms in the subthreshold range $0 < V_{GS} < +0.5$V, and the linear and exponential $(\partial/\partial y)(E_X)^2$ terms in the strong channel current range, $V_{GS}<0$ for the hole channel and $V_{GS}>+0.5$V for the electron channel where the two parts of the pair both have large values but opposite in sign to give near complete cancellation of the two terms in the two voltage ranges.

The output characteristics are shown in Figs. 4, 5, and 6 for positive V_{DS} or electron channel dominant initially. i. e. when V_{DS} increases from 0, because hole channel would overwhelm after the electron channel current saturates when V_{DS} continues to increase as explained below. Identi-

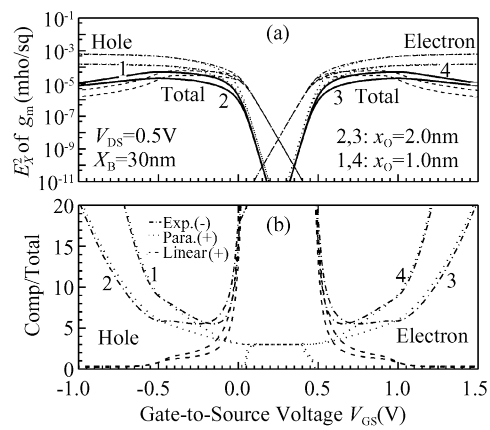

Fig. 14 Similar to Fig. 13 but for the transconductance, g_m.

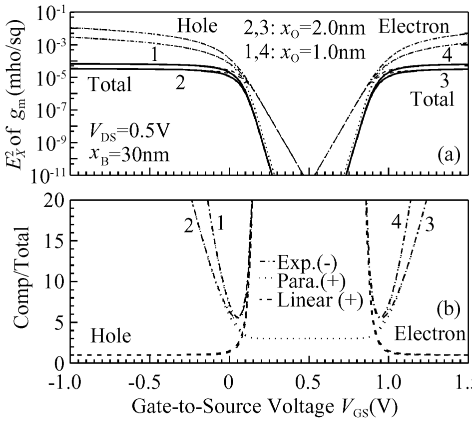

Fig. 15　Similar to Fig. 14 but for the output or drain conductance，g_d.

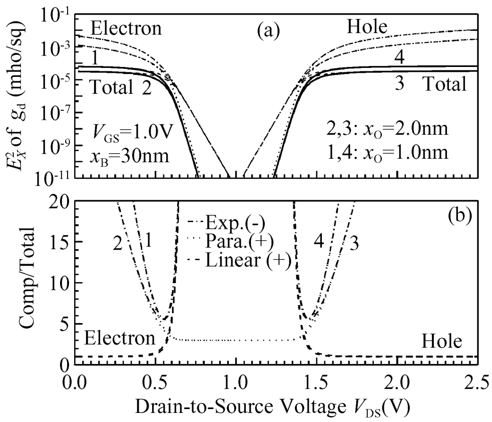

Fig. 17　Similar to Fig. 16 but for the output or drain conductance，g_d.

cal curves and points are obtained but not presented in this paper for negative V_{DS} or hole channel initially dominant. Figures 4 (a)，4 (b) and 4 (c) show the drain voltage (V_{DS}) dependences corresponding to the gate voltage dependences shown in Figs. 1 (a)，1 (b) and 1 (c)，except the constant parametric gate voltage is now set at $V_{GS} = +1.0V$，which shifts the onset of the parabolic drift saturation current of the hole channel to $V_{DS\text{-sat-hole}} = +1.5V$ as indicated in Fig. 4 (a). Figure 4 (b) shows clearly the importance of the $(\partial/\partial y)(E_X)^2$ contribution，rising to a fraction of 0.25 or 25% of the total channel current when the parabolic electron drift current saturates，$V_{DSsat\text{-}electron} = V_{GS} - V_{GSth\text{-}electron} = +1.0V - 0.5V = +0.5V$. As indicated in Fig. 4 (c)，the deviations of the present Drift-Diffusion theory (DD) are still less than 10^{-12}% from the Electrochemical Potential Gradient (ECP) theory of [7]，and the deviations are purely numerical from the 64-bit finite precision of the computer hardware and the Fortran software.

The output characteristics in Figs. 5 and 6 are the drain voltage dependencies of the drain conductance and transconductance characteristics. They are similar to the gate voltage dependencies just shown and described on Figs. 2 and 3，therefore，they are not describe further.

The base and oxide thickness dependences are shown in Figs. 7 to 18，which further delineate the importance of the three $(\partial/\partial y)(E_X)^2$ component terms (linear，parabolic，and exponential). These

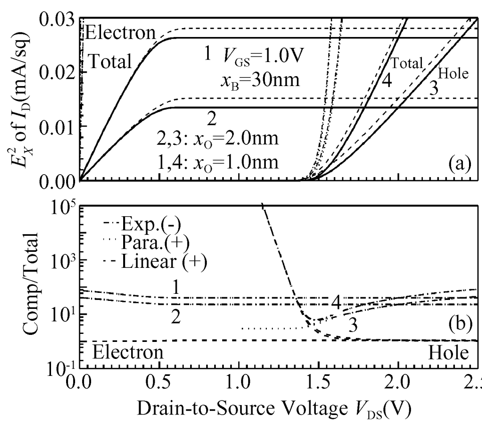

Fig. 16　These two parts of the figure are similar to those in Fig. 13. They give the effects of oxide thickness，x_O = 1.0nm and 2.0nm，on contribution from the three $(\partial/\partial y)(E_X)^2$ components，Exponential，Parabolic，and Linear to the electron and hole channel currents. (a) Similar to that given in Fig. 4 (a) except that the $(\partial/\partial y)(E_X)^2$ term is shown in place of the drift and diffusion components. (b) The contributions of the three components of the $(\partial/\partial y)(E_X)^2$ as a fraction of the total $(\partial/\partial y)(E_X)^2$ contribution.

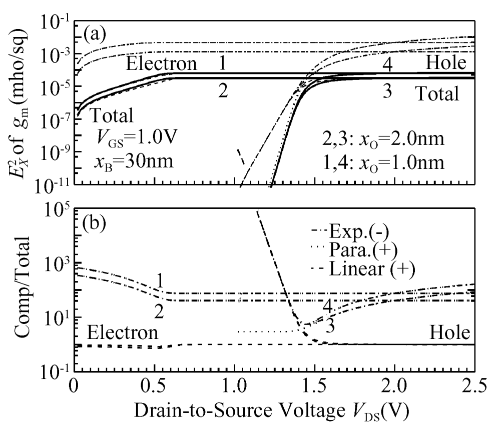

Fig. 18　Similar to Fig. 17 but for the transconductance g_m.

are illustrated in part (a) of these 12 figures. The fractional contribution of each of the three terms to the total, is shown in part (b). These suggest that very accurate compact models can be developed by assuming the channel current and conductances are proportional to the base to oxide thickness ratio, (x_B/x_O), with a higher order term from the oxide thickness. The underlying device physics is described in the figure discussions.

The six figures, Figs. 7 to 12, show the same families of characteristics as Figs. 1 to 6, at the same gate oxide thickness, $x_O = 1.5$nm, but at two different base thicknesses, $x_B = 3$nm and 300nm, while Figs. 1 to 6 are for $x_B = 30$nm. In contrast, Figs. 7 to 12, shows the relative importance of the three components of the $(\partial/\partial y)(E_X)^2$, which were given by Eq. (11) and labeled in the figures as L (for Linear), P (for Parabolic) and E (for Exponential). These six figures also illustrate two base-thickness effects on the total contribution from the $(\partial/\partial y)(E_X)^2$ to the electron and hole channel currents: (1) the tremendous reduction, ~100 (the x_B ratio of 300nm/3nm), over the entire voltage ranges from strong surface channel to subthreshold; and (2) the smaller reduction of the hole and electron channel currents and conductances in thinner base of very strong surface channel range of V_{GS}, due to closer proximity of the second gate to the first gate.

The oxide thickness dependences are shown by the last six figures, Figs. 13 to 18, for x_O = 1.0nm and 2.0nm, while Figs. 1 to 6 has x_O = 1.5nm, both sets with base thickness, $x_B = 30$nm. The main results are (1) the strong electron and hole channel currents are nearly inversely proportional to the oxide thickness, as expected from the larger electron and hole channel charges and hence currents induced by the thinner gate oxide at a given gate voltage, and (2) the subthreshold currents are not affected by the oxide thickness, because the oxide is electrically thin compared with the base-thickness and the Debye length, thus, the applied gate voltage is mostly used to create the space-charge layer over the entire thickness, x_B, of the pure base.

Acknowledgment We thank Professor Xing Zhou (Nanyang Technological University, Singapore) for asking the senior author back into the compact modeling community after more than 40-years of absence, by attending the 4th annual Workshop of Compact Modeling on May 10, 2005, which Dr. Zhou founded four years earlier in 2001, and for asking us to extend our bench-mark analytical solution efforts of MOS transistors to include the latest and future nanometer technology such as the double-gate and thin-base described in this report. We thank Professor Chenming Hu (University of California, Berkeley) for a copy of the digital slides of his invited talk cited in Ref. [1]. We also thank Professors Gennady Gildenblat (Arizona State University) and Mitiko Miura-Mattausch (Hiroshima University) and Dr. Colin McAndrew (Freescale Semiconductor Corporation), and Drs. Jin Cai, Tak H. Ning, Lewis M. Terman, and Hwa-Nien Yu (IBM Thomas J. Watson Research Center) for encouragements to undertake these investigations and for their comments and suggestions. We further thank Professors Marcel D. Profirescu (Univeristy Politechnica of Bucharest, Romania), Adelmo Ortiz-Conde and Francisco J. Garcia Sanchez (Universidad Simon Bolivar, Venezuela), Juin J. Liou (University of Central Florida, USA) and Professors Xing Zhou and Cher Ming Tan (Nanyang Technological University) for inviting us to present our results at their IEEE EDS Mini-Colloquium, ICCDCS, INEC and WCM conferences.

References

[1] Chenming Hu, "From CMOS to Nanotechnology," Keynote, 17th Annual IEEE/SEMI Advanced Semiconductor Manufacturing Conference, May 22—24, 2006, Boston, Massachusetts.

[2] T. Hoffmann, G. Doornbos, I. Ferain, N. Collaert, P. Zimmerman, M. Goodwin, R. Rooyackers, A. Kottantharayil, Y. Yim, A. Dixit, K. De Meyer, M. Jurczak, S. Biesemans, "GIDL (Gate-Induced Drain Leakage) and Parasitic Schottky Barrier Leakage Elimination in Aggressively Scaled HfO_2/TiN FinFET Devices," IEDM Technical Digest, Dec. 2005, 743—746.

[3] A. Ortiz-Conde, F. J. Garcia-Sanchez, J. Muci, S. Malobabic, J. Liou, "A Review of Core Compact Models for Undoped Double-Gate SOI MOSFETs," IEEE Trans Elec Dev, 54(1), 131—139, January 2007.

[4] Chih-Tang Sah and Bin B. Jie, "Double-Gate Thin-Base MOS Transistor: The Correct Theory," and Bin B. Jie and Chih-Tang Sah, "Double-Gate Thin-Base MOS Transistor: Characteristics for the Short Channel," Late-News Papers Presented on May 23, 2007 at the Workshop on Compact Modeling (WCM20070523) of the NSTI Nanotechnology Conference and Trade Show, May 22—24, 2007, the Nano Science and Technology Institute, Cambridge, MA 02139, USA. http://www.nsti.org/Nanotech2007/WCM2007/.

[5] Chih-Tang Sah and Bin B. Jie, "Bipolar Theory of MOS

Field-Effect Transistors and Experiments，” Chinese Journal of Semiconductors，28(10)，1497—1502，October 2007.

[6] Bin B. Jie and Chih-Tang Sah，“Bipolar Theory of MOS Field-Effect Transistors and Experiments，” Invited Paper，IEEE Electron Device Society，Mini-Colloquium NADE—Nano-electronic Devices Present and Perspectives，Sinaia，Bucharest，Romania，October 14，2007. Twenty-eight Presentation Slides in Conference Proceedings. Editor：Marcel D. Profirescu，P. O. Box 57-112，Bucharest 74500，Romania. profires@edil. pub. ro

[7] Chih-Tang Sah and Bin B. Jie，“The Bipolar Field-Effect Transistor：I. Electrochemical Current Theory（Two-MOS-Gates on Pure-Base），” Chinese Journal of Semiconductors，28(11)，1661—1673，November 2007.

[8] H. S. Fu and C. T. Sah，“A Distributed-Gate Bistable MOS Transistor，” Solid-State Electronics 14(9)，799—804，September 1971. Figures of this article presented in one slide in [6].

[9] Chih-Tang Sah and Henry C. Pao，“The Effects of Fixed Bulk Charge on the Characteristics of Metal-Oxide-Semiconductor Transistor，” IEEE Trans Elec Dev，13(4)，410—415，April 1966.

[10] Henry C. Pao and Chih-Tang Sah，“The Effects of Diffusion Current on the Characteristics of MOS Transistors，” Solid-State Electronics，9(10)，927—938，October 1，1966. This is frequently referred to as 1966-Pao-Sah. However，the most extensive analytical approximation efforts by compact model developers in the last 40 years were all spent on the voltage equation first given in the 1965-Sah-Pao[9]. Reference to both [9] for the voltage equation and [10] for the current equation has recently been made as 1966-Sah-Pao by Gildenblat and other recent developers of compact MOS transistor models[11,12]. The existence of two separate articles [9,10] one for each of the two equations was first noticed recently by Xing Zhou.（Private Communication May 2005.）

[11] Chih-Tang Sah and Bin B. Jie，“A History of MOS Transistor Compact Modeling，” Keynote. Technical Proceedings Workshop on Compact Modeling（WCM），Abstract on pp. 1—2 and full text on pp. 349—390. Editors：Xing Zhou，Matthew Laudon and Bart Romanowicz. NSTI Nanotech 2005. The NSTI Nanotechnology Conference and Trade Show，May 8—12，2005. Nano Science and Technology Institute，Cambridge，MA 02139，USA. ＃PCP05040394.
On-line：http：//www. nsti. org/publ/Nanotech2005WCM/1429. pdf

[12] J. Watts，C. McAndrew，C. Enz，C. Galup-Montoro，G. Gildenblat，C. Hu，R. van Langevelde，M. Miura-Mattausch，R. Rios and C. T. Sah，“Advanced Compact Models for MOSFETs，” Technical Proceedings Workshop on Compact Modeling（WCM），3—12. Editors：Xing Zhou，Matthew Laudon and Bart Romanowicz. NSTI Nanotech 2005. The NSTI Nanotechnology Conference and Trade Show，May 8—12，2005. Nano Science and Technology Institute，Cambridge，MA 02139，USA. ＃PCP05040394. On-line：See [11] above.

[13] Bin. B. Jie and Chih-Tang Sah，“Evaluation of Surface-Potential-Based Bulk-Charge Compact MOS Transistor Model，” IEEE Trans Elec Dev，52(8)，1787—1794，Aug 2005.

[14] Bin B. Jie and Chih-Tang Sah，“Accuracy of Surface-Potential-Based Long-Wide-Channel Thick-Base MOS Transistor Models，” IEEE Trans Elec Dev，54(8)，1897—1909，August 2007.

[15] Chih-Tang Sah，“Space Charge Theory of the MOS Transistor，” Intel Grant Report，Dec. 12，1996. Derivations were reproduced and presented in [13] and [14].

[16] G. Gildenblat，X. Li，H. Wang，W. Wu，A. Jha，R. van Langevelde，A. J. Scholten，G. D. J. Smit，and D. B. M. Klaassen，“Theory and Modeling Techniques Used in the PSP Model”，Technical Proceedings Workshop on Compact Modeling（WCM），604—609，May 9，2006，Boston，Massachusetts，USA. On-line presentation slides：http：//www. nsti. org/Nanotech2006/ WCM2006/WCM2006-GGildenblat. pdf（See Slide 24）.

[17] W. Z. Shangguan，Xing Zhou，K. Chandrasekaran，Zhaomin Zhu，S. C. Rustagi，S. B. Chiah，and G. H. See，“Surface-Potential Solution for Generic Undoped MOSFETs with Two Gates，” IEEE Trans Elec Dev，54(1)，169—172，January 2007.

[18] Mitiko Miura - Mattausch and Hermann Jacobs，“Analytical Model for Circuit Simulation with Quarter Micron Metal Oxide Semiconductor Field Effect Transistors：Subthreshold Characteristics”，Japan J. Appl. Physics，29，L2279—2282，1990.

双极场引晶体管：II. 飘移扩散理论（双 MOS 栅纯基）*，**

薩支唐[1,2,3,†]　揭斌斌[3,†]

（1 中国科学院外籍院士，北京　100084）
（2 佛罗里达大学，佛罗里达州，Gainesville　FL32605，美国）
（3 北京大学，北京　100871）

摘要： 本文描述双极场引晶体管（BiFET）飘移扩散理论，包括薄纯基上两个等同金属氧化物硅（MOS）栅.把两维晶体管分解成两个一维问题，以表面势为参变量，得到解析方程.提供实用硅基和氧化层厚度范围内，随直流电压变化，输出和转移电流和电导总量和飘移扩散分量.显著部分的飘移电流来自横向电场平方的纵向梯度.

关键词： 双极场引晶体管理论；MOS 场引晶体管；双极结型晶体管；同时并存空穴电子表面沟道和体积沟道；表面势；横向电场的纵向梯度

PACC： 7340Q　　**EEACC：** 2560S；2560B

中图分类号： TN386.1　　**文献标识码：** A　　**文章编号：** 0253-4177(2007)11-1849-11

* 该研究及揭斌斌由 CTSAH Associates（CTSA）资助.CTSA 由已故的薩夫人张淑南创建.

** 薩支唐写成此摘要基于揭斌斌的现代语初稿.感谢潘胜和北京大学原物理系教师赵立群和潘桂明的修改建议.

† 通信作者.Email：bb_jie@msn.com and tom_sah@msn.com

2007-10-31 收到，2007-11-10 定稿